Controlling Factors on Droplets Uniformity in Membrane Emulsification: Experiment and Modeling Analysis

Dong-Xia Hao,[†] Fang-Ling Gong,[†] Guo-Hua Hu,[‡] Yong-Jiang Zhao,[†] Guo-Ping Lian,[§] Guang-Hui Ma,*[,†] and Zhiguo Su[†]

National Key Lab of Biochemical Engineering, Institute of Process Engineering, Chinese Academy of Sciences, Beijing 100080, People's Republic of China, Laboratory of Chemical Engineering Sciences, CNRS-ENSIC-INPL, 1 rue Grandville BP 20451, 54001 Nancy, France, and Institut Universitaire De France, Maison Des Universités, 103 Boulevard Saint-Michel, 75005 Paris, France, and Unilever R&D Colworth, Sharn Brook, Bedfordshire MK44 1LQ, United Kingdom

The membrane emulsification process is attracting great interest in many industrial fields. For optimization and scaling up of the emulsification process, controlling the emulsion uniformity using monitoring process and membrane parameters is especially important. In this study, the effects of phase physical property (viscosity, interfacial tension), and operation conditions (trans-membrane pressure shear stress), on droplet size distribution of an oil-in-water (o/w) emulsion were systemically investigated by membrane emulsification experiments with a cross-flowing continuous phase. Inspired by the idea that droplet spontaneous formation is one of the most important mechanisms to form a uniform emulsion, a simple model based on torque balance equations by describing the variable force torques on droplet formation process was proposed to predict experimental tendencies. The experiment phenomena showed a good coincidence with model prediction. The following experiment conditions were found to facilitate the production of uniform droplets: (1) low cross-flow velocity of the continuous phase, (2) low transmembrane pressure, (3) high viscosity of the dispersed phase, and (4) an emulsifier with great ability and rapid rate to decrease interfacial tension.

1. Introduction

Emulsions with size uniformity and size controllability have presented distinctive advantages in many industrial applications, such as stable emulsion in food manufacture, size-targeted microcapsules in drug delivery, and uniform microspheres media in chromatographic separations.[1–3] For large-scale emulsion production, the most commonly techniques are rotor−stator or homogenizer systems, in which emulsion droplet formation is mainly dependent on the exersion of strong external dissipated energy into fluid mixtures. Because the dissipated energy cannot be controlled homogeneously and efficiently, an emulsion with a broad size distribution is often obtained. A great amount of work has focused on exploring new devices with milder and more-controllable dissipating technique to produce a uniform emulsion. Membrane emulsification has been addressed recently by alternative techniques, such as those by which the phase to be dispersed could grow into uniform droplets separately at highly uniform membrane pores with the help of a gentle and accurately controlled driving force.[4] The distinguishing feature of this technique is that the resulting droplet size is easily controlled by the membrane pore rather than by the turbulent shearing flow; therefore, this technique presents many advantages, such as a narrow size distribution of droplets, a lower energy requirement, and suitability for the emulsification of shear- or temperature-sensitive components.

Membrane emulsification is a two-liquid phase flow process, in which the phase to be dispersed is pressed through the membrane inner channel, droplets grow at the membrane pore, and, after reaching a certain size, the droplets are carried away by continuous phase flowing. In this microscopic flow process, different parameters take combined actions at multiscales and with different magnitude, such as interfacial surface properties (diffusion, surface tension, and viscosity of two phases) and macroscopic operation conditions (velocity or pressure of the dispersed phase, velocity of the continuous phase velocity).[5] The effects of these various parameters on the final emulsion droplet size have been analyzed experimentally by many researchers.[6–9] Besides, numerical studies with various calculation methods have also been constructed to describe formation of droplet and predict droplet size, such as force and torque balances,[10–12] surface free-energy minimization,[13,14] computation fluidic dynamics (CFD),[15] the lattice Boltzmann method,[16] and the phase flow method[17] recently. Here, from another point of view, we intended to determine how the aforementioned parameters make control of emulsion uniformity in membrane emulsification by experiment and theoretical approaches. The influence of operation conditions, the physical properties of the two phass and membrane parameters on the droplet formation and emulsion uniformity will be investigated systemically in emulsification, and torque balance model will be used to analyze and predict the experiment trend, because of its versatility in incorporating almost all of the aforementioned fundamental parameters in the membrane emulsification process.

2. Experimental Section

2.1. Materials. Deionized water was used as the continuous phase. The dissolved emulsifiers were sodium dodecyl sulfate (SDS, chemical grade, Beijing Jingqiu Chemical Industry Co., Ltd.), poly(vinyl alcohol) (PVA, degree of polymerization 1700, degree of hydrolysis, 88.5%) kindly provided by Kuraray (Japan), and polyoxy-ethylene (20) sorbitan monolaurate (Tween20, SERVA Eletrophoresis GmbH). Soybean oil (com-

* To whom correspondence should be addressed. Fax: 80-10-82627072. E-mail address: ghma@home.ipe.ac.cn.

[†] National Key Lab of Biochemical Engineering, Institute of Process Engineering, Chinese Academy of Sciences.

[‡] Laboratory of Chemical Engineering Sciences, CNRS-ENSIC-INPL and Institut Universitaire De France, Maison Des Universités.

[§] Unilever R&D Colworth.

10.1021/ie8000315 CCC: $40.75
Published on Web 06/11/2008

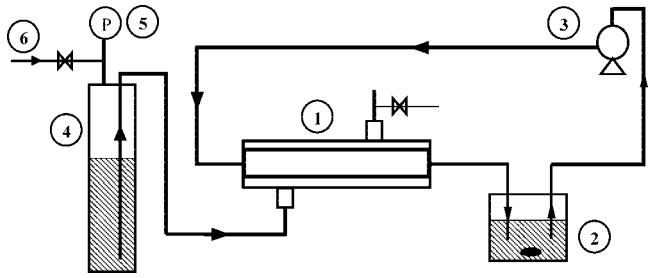

Figure 1. Diagram of equipments in membrane emulsification. Figure legend: (1) MPG module, (2) emulsion storage tank, (3) recirculation pump, (4) storage tank of dispersed phase, (5) pressure gauge, and (6) nitrogen source.

Table 1. Properties of the Experimental Systems for Membrane Emulsification[a]

system (dispersed phase)	γ_0 (mN/m)	γ_e (mN/m)	viscosity (mPa·s)
soybean oil	17.10	4.81 (2% SDS)	61.114
		7.55 (2% Tween20)	
		13.08 (2% PVA)	
liquid paraffin	46.20	6.36 (2% SDS)	10.612
		8.41 (2% Tween20)	
		20.12 (2% PVA)	
divinylbenzene	15.64	4.55 (2% SDS)	1.967

[a] Other parameters: $t^* = 0.245$, $n = 2.146$ for SDS 2% aqueous solution; $t^* = 0.302$, $n = 1.189$ for Tween 2% aqueous solution.

mercial grade, Northsea Oils and Grains Industries Co., Ltd., China), Divinylbenzene (DVB, 55 wt%, Dongda Chemical Engineering Group Co., China), liquid paraffin (analysis-grade, Beijing Chemical Reagents Company), were used as the dispersed phase respectively.

2.2. Emulsification. The emulsion was prepared using the Microporous glass membrane module (MPGNA-I,ISE Chemical Co.), as shown in Figure 1. The glass membrane was an annulus cylinder (inner diameter of ID = 8 mm, length of $L = 170$ mm) with a pore size of 5.2 μm. The dispersed phase (the oil phase) was pressed through the pores of the membrane into the aqueous phase continuously by applying nitrogen gas pressure, which is set to 10% slightly higher above the critical pressure (P_γ^0). The continuous phase flow (the water phase) was controlled with a peristaltic pump, one of which (6−600 rpm, Masterflex, Cole-Parmer Instrument Co.USA) was used at the velocity of continuous phase below 1m/s, and another (CF50, pump, Hanatsuka) was used at the velocity of continuous phase above 1m/s.

2.3. Determination of Droplet Size Distribution. The droplet diameters were immediately observed under an XSZ-H_3 optical microscope (Coic, China) after emulsification for 30 min, to avoid coalescence between the suspended droplets. The diameters of at least 300 droplets were counted to calculate the average diameter and the size distribution, which is expressed by a CV value and is defined as follows:

$$\mathrm{CV} = \frac{\left[\sum_{i=1}^{n} \frac{(d_i - d)^2}{n}\right]^1}{d}$$

where d_i is the diameter of the ith microsphere, d the average diameter, and n the total number of the microspheres counted.

2.4. Determination of Viscosity. The viscosity of both phases is determined by a rotational rheometer (L-90, Mechanical and Electric Plant of Tongji University), based on the formula

$$\eta \quad (\mathrm{mPa \cdot s}) = \frac{\tau\ (\text{shear stress})}{D\ (\text{shear rate})}$$

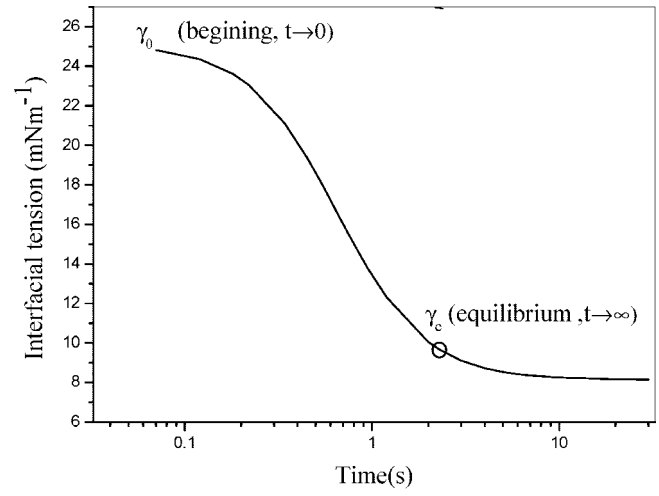

Figure 2. Typical dynamical interfacial tension course.

by measuring the torques on a rotor in Couette flow at 25 °C. Divinylbenzene, liquid paraffin, and all the continuous phases were measured under the condition of a No. 3 rotor; soybean oil was measured under the conditions of a No. 2 rotor. The measurement results are listed in Table 1.

2.5. Determination of Dynamic Interfacial Tension. Figure 2 shows a typical dynamic interfacial tension course between a dispersed phase and a continuous phase[18] in membrane emulsification, which can be described by the following analytical expression:[19]

$$\gamma_t(t) = \frac{\gamma_0 + \gamma_e(t/t^*)^n}{(1 + t/t^*)^n}$$

where γ_0 is the interfacial tension between pure water and the dispersed phase, γ_t is the interfacial tension between the dispersed phase and the continuous phase at a specific time t, whereas γ_e is the mesoequilibrium interfacial tension (when γ_t does not change much with t, as determined by experimental data), and t^* and n are constants that are related to the emulsifier concentration and its molecular structure.[19] In this study, the values of t^* and n for the SDS and Tween20 solutions were adjusted by a nonlinear fitting routine that was based on the dynamic interfacial tension data reported by Schuberts et al. As for PVA without published data, the values of t^* and n are defined as the same value with the SDS solution. The value of γ_0 and γ_e between the two phases were respectively measured via the pendant drop method, aided by a video-image digitization technique, as shown in Table 1. The water phase was injected slowly, using a needle, into the oil phase under a constant pressure and was monitored by an OCA contact angle system (Dataphysics, Germany); the interfacial tension then was calculated from the video image.

3. Results and Discussions

3.1. Mechanisms of Droplet Detachment Determining the Emulsion Uniformity. It has been demonstrated that final emulsion uniformity is mainly dependent on droplet detachment behavior in membrane emulsification, except in the cases where the polydispersity of the emulsion is caused by instability of the emulsion and wettability of the dispersed phase, relative to the membrane. Two mechanisms are involved in droplet detachment, i.e., shear-induced droplet formation (SHE) and spontaneous transformation-based droplet formation (STB).[20,21] The mechanism of SHE describes the situation where the droplet

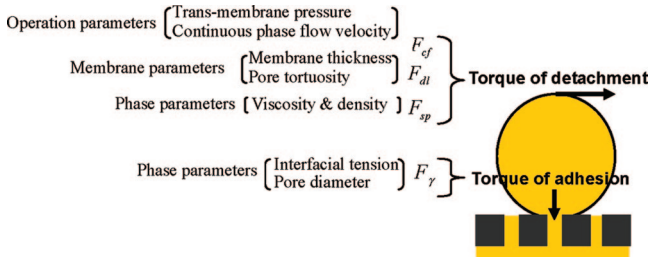

Figure 3. Torques on the global droplet.

must be detached by shear force of cross-flow or rotary flow of the continuous phase. The mechanism of STB describes the situation where the droplet breaks off without any additional shearing and just by the variation of interfacial free energy.

Kobayashi and Sugiura have demonstrated that droplet detachment driven by the mechanism of STB resulted in the production of a more-uniform emulsion than that driven by the mechanism of SHE.[22–24] Using microchannels with a oblong or terrace outlet, emulsions with a narrow size distribution were produced as a result of the microcosmic instability of the elongated droplet interface in its detachment process. In this case, droplets were observed to spontaneously break off from the outlet without any external cross-flow. However, using microchannels with a circular outlet, emulsion droplets with a wider size distribution were produced. In this case, microscopic investigation shows that it seems to be difficult to detach the droplets from the circular outlet. Their detachments must be driven by a strong drag force of continuous-phase flow, and the droplets size and distribution was significantly influenced by the operating conditions, such as fluctuation of flow field of continuous phase at a microscale.

A Shirasu porous glass (SPG) membrane with a apore geometry composed of tortuous ellipsoidal cylinders has characteristics between those of the circular and elongated outlets. Consequently, both mechanisms of spontaneous formation and shearing formation were observed to take action under different operating conditions via microscope visualization of SPG membrane emulsification.[20] Such an experiment also found that the low flux of dispersed phase and flow rate of continuous phase resulted in the spontaneous droplet detachment behavior, which produced a more-uniform emulsion than shearing formation behavior.

3.2. Modeling of the Droplet Detachment. According to the aforementioned analysis, the difference between the two mechanisms is dependent on the difficulty of droplet detachment. Such difficulties can be indirectly reflected by macroscopic forces, or, specifically, the mechanical torques that are being exerting on a global droplet. Figure 3 presents a framework of all the forces and torques acting on a droplet, which can be divided into two groups—detachment torques and adhesion torques—based on their respective roles to drive droplets off the pore and hold droplets on the pore. In the following subsections, we will construct a multivariable torque model that associates operating parameters, membrane parameters, and the physical-chemistry property of two phases and examine their respective influences on droplet detachment mechanism.

(i) Force Torque Acting on the Global Droplet. The main forces on the droplet have been identified in the literature[25,26] and are described as follows. The major retaining force in the torque of adhesion is theinterfacial tension force (F_γ), which represents the effects of the dispersed-phase adhesion on the pore opening and is a function of the dynamic interfacial tension $\gamma(t)$:

$$F_\gamma = \pi d_p \gamma(t) \tag{1.1}$$

The static pressure difference force (F_{sp}) is a force that is caused by the pressure difference between the dispersed phase and the continuous phase at the membrane surface. In quasi-static state, it is described as

$$F_{sp} = (P_i - P_o)A_p = \Delta P_\gamma A_p = \pi\gamma(t)\left(\frac{d_p^2}{d_{dr}}\right) \tag{1.2}$$

where A_p is the cross-sectional area of the droplet neck at the pore and, here, is approximately assumed to be equal to the area of the pore, and d_{dr} is the dynamic droplet diameter, which increases until the droplet detachs from the pore. The cross-flow drag force (F_{cf}) is created by the continuous phase flowing past the droplet parallel to the membrane surface, according to Stokes' equation in a simple shear flow, which is assumed that the droplets are formed in the laminar sublayer.[26]

$$F_{cf} = 3\pi\mu_c d_{dr}\mu_c \tag{1.3}$$

The dynamic lift force (F_{dl}) results from the asymmetric velocity profile of the continuous phase near the droplet and is defined as

$$F_{dl} = \frac{0.761\tau_w^{1.5} d_{dr}^3 \rho_c^{0.5}}{\mu_c} \tag{1.4}$$

where the shearing force (τ_w) is controlled by the velocity of the continuous phase (u_c)[25] and can be deduced based on the definition of the Fanning friction factor:

$$\tau_w = f\left(\frac{\rho_c u_c^2}{2}\right) \tag{1.5}$$

where ρ_c is the density of continuous phase, u_c the flow velocity of the continuous phase, and f a dimensionless factor defined by the Reynolds number (Re) as follows:

$$f = \begin{cases} \dfrac{16}{Re} & (Re < 2000) \\ 0.00140 + \dfrac{0.125}{Re^{0.32}} & (2\times10^3 < Re < 3\times10^6) \end{cases} \tag{1.6}$$

where $Re = \rho_c u_c D/(\mu_c D)$ is the inner diameter of the crossflow channel (membrane channel) and μ_c is the viscosity of the continuous phase.

The forces of buoyancy and gravity (F_{BG}) can be described as the density difference between the two phases:

$$F_{BG} = F_B - F_G = (\rho_c - \rho_d)gV_d \tag{1.7}$$

The linear momentum force (F_m) is caused by flow movement of a mass of the dispersed phase out from the pore outlet:

$$F_m = \int_{A_p} \rho_d v_d^2 \, dA = \frac{\pi}{4}\rho_d u_d^2 d_p^2 \tag{1.8}$$

Among these forces, F_γ is the holding force, whereas F_{sp}, F_{cf}, F_{BG}, F_{dl}, and F_m are detaching forces. Because of the linear momentum force (F_m), the buoyancy and gravity force (F_{BG}) can be neglected, because they are approximately 6−8 orders of magnitude smaller than other forces after calculation; all the torques shown in Figure 3 can be grouped as follows.

Torque of adhesion, $T_{adhesion}$:

$$T_{adhesion} = F_\gamma\left(\frac{d_p}{2}\right) = T_{adhesion}[\gamma(t), d_p] \tag{1.9}$$

Torque of detachment, T_{detach}:

$$T_{\text{detach}} = (F_{\text{sp}} + F_{\text{dl}})\frac{d_{\text{p}}}{2} + F_{\text{cf}}h = T_{\text{detach}}[\gamma(t), d_{\text{p}}, h(t), d_{\text{dr}}(t), \tau_{\text{w}}(u_{\text{c}}), \rho_{\text{c}}, \mu_{\text{c}}] \quad (1.10)$$

where h represents the growing height of droplet at membrane pore, and, accordingly, both torques can be determined as functions of the aforementioned parameters. Among them, the physical chemistry properties of the two phases, such as interfacial tension $\gamma(t)$ and viscosity, can be measured in section 2, and other parameters such as droplet diameter growth $d_{\text{dr}}(t)$ and the related height of the droplet $h(t)$ are the dynamic variables and time-dependent with the development of the droplet growth, which is determined in the following section (section ii) by further association with other parameters.

(ii) Droplet Growth Controlled by Transmembrane Pressure of Dispersed Phase in Membrane Channel. In a droplet that is forming at the membrane pore, the dispersed-phase flow rate through the pores of the membrane (Q_{dr}) may be assumed based on Darcy's law and the Hagen−Poiseuille equation as follows:[10]

$$Q_{\text{dr}} = \frac{\pi d_{\text{p}}^4 P_{\text{ef}}}{128\xi\mu_{\text{d}}L} \quad (2.1)$$

where d_{p} is the membrane pore size (here, a value of 5.2 μm has been used), ξ is the pore tortuosity (here, an approximate value of 2.1 has been used, which was measured and calculated using hydraulic membrane resistance by Vladisavljevic[6]), μ_{d} is the viscosity of the dispersed phase, and L is the membrane thickness. P_{ef} is the effective transmembrane pressure necessary to control the dispersed phase; it is defined as the difference of two pressures,

$$P_{\text{ef}} = P_{\text{trm}} - P_{\gamma} = P_{\text{trm}} - \frac{4\gamma(t)}{d_{\text{dr}}} \quad (2.2)$$

where P_{trm} is the transmembrane pressure applied in emulsification between each side of the membrane, and P_{γ} is the capillary pressure.

Because the dynamic droplet volume V_{d} can be related to the dispersed-phase flow rate Q_{dr} by the following continuity equation of the dispersed phase,

$$\frac{dV_{\text{dr}}}{dt} = Q_{\text{dr}}[h(t), \gamma(t)] \quad (2.3)$$

the volume of the droplet, as a spherical cap, can be calculated, using the height of the droplet $h(t)$, as follows:

$$V_{\text{dr}}[h(t)] = \frac{1}{6}\pi h(t)\left(\frac{3}{4}d_{\text{p}}^2 + h(t)^2\right) \quad (2.4)$$

The dynamic height of droplet $h(t)$ can thus be deduced using eqs 2.3, 2.4, and 2.1:

$$\frac{dh}{dt} = \frac{\left(\frac{dV_{\text{d}}}{dt}\right)}{\left(\frac{dV_{\text{d}}}{dh}\right)} = \frac{\left(\frac{dV_{\text{d}}}{dt}\right)}{8\pi(d_{\text{p}}^2 + 4h^2)} = \frac{d_{\text{p}}^4}{16\mu_{\text{d}}\xi L}\left[\frac{P_{\text{tm}}}{d_{\text{p}}^4 + 4h^2} - \frac{16\gamma(t)h}{(d_{\text{p}}^2 + 4h^2)^2}\right] \quad (2.5)$$

The droplet diameter ($d_{\text{dr}}(t)$) can also be described by the height of droplet $h(t)$:

$$\frac{d_{\text{dr}}}{2} = \frac{(d_{\text{p}}/2)^2 + h^2}{2h} \quad (2.6)$$

Therefore, the droplet growth, $d_{\text{dr}}(t)$, can be deduced from eqs 2.5 and 2.6:

$$\frac{d(d_{\text{dr}})}{dt} = \frac{d(d_{\text{dr}})}{dh}\frac{dh}{dt} = \left[1 - \frac{1}{4}\left(\frac{d_{\text{p}}^2}{h^2}\right)\right]\frac{d_{\text{p}}^4}{16\mu_{\text{d}}\xi L}\left[\frac{P_{\text{tm}}}{d_{\text{p}}^4 + 4h^2} - \frac{16\gamma(t)h}{(d_{\text{p}}^2 + 4h^2)^2}\right] \quad (2.7)$$

The initial conditions for eqs 2.6 and 2.7 are established according to the Laplace equation, with the initial interfacial tension and critical pressure, and $h(0)$ is also determined by eq 2.6.

$$d_{\text{dr}}(0) = \frac{4\gamma(0)}{P_{\gamma}^0}$$

and

$$P_{\gamma}^0 = \frac{16\gamma(0)h(0)}{d_{\text{p}}^2 + 4h(0)^2}$$

Based on all the aforementioned facts, the torque models on the droplets are constructed by a coupling of operating parameters, membrane parameters, and the physicochemistry properties of the two phases, i.e., $T_{\text{adhesion}}[\gamma(t),d_{\text{p}}]$ and $T_{\text{detach}}[\gamma(t),d_{\text{p}},d_{\text{dr}}(P_{\text{trm}},\xi,L,\mu_{\text{d}},t),\tau_{\text{w}}(u_{\text{c}}),\rho_{\text{c}},\mu_{\text{c}}]$. When these two torques are balanced (i.e., $T_{\text{adhesion}} = T_{\text{detach}}$, the droplet begins to detach. It was found by one-hole droplet formation experiments where, at the balance point, if the adhesion torque (or interfacial tension) was very large, the droplet would be difficult to break off and a larger detachment torque (or shearing stress) was needed.[28] In this case, the droplet had a tendency to be dragged by the SHE mechanism, instead of being dragged by the STB mechanism. Therefore, in this study, it is proposed that torques at the balance point may act as a comparison criterion for estimating the transformation of the droplet detachment mechanism and, thus, the emulsion uniformity. Droplet diameter growth $d_{\text{dr}}(t)$, shear force τ_{w}, and other related emulsification parameters can be associated with the aforementioned torque models. Therefore, the disturbances of these parameters on torques can be calculated to predict their influences on emulsion uniformity.

3.3. Influence of Continuous Phase Flow on Emulsion Uniformity. Continuous phase flow is a fundamental process parameter to determine membrane emulsification characteristics, because wall shear stress caused by the continuous phase is a major force to drive the droplets that are departing from the membrane pore. The effects of different continuous phase flow rates on emulsion uniformity were investigated by oil-in-water (o/w) emulsification experiments. Figure 4 shows that the distribution of droplet size (CV, expressed as a percentage) can remain narrow over a wide range of the continuous phase flow rates (from 0.188 m/s to 1.85 m/s). With further increases in continuous phase flow from 1.85 m/s to 3.95 m/s, the droplet size distribution quickly changed to broad.

Figure 5 describes the development of two types of torque that we calculated: adhesion and detachment. Because adhesion torque is a function of dynamic interfacial tension, the curve of adhesion torque presents the same changes with dynamic interfacial tension, which decreases sharply at the beginning and then comes to equilibrium in regard to droplet formation. Comparatively, the detachment torque curve also presents a decreasing trend with droplet formation time. The two types of torque become balanced at the intersection point of curves. This shows that, as the continuous phase flow increases from 1.85

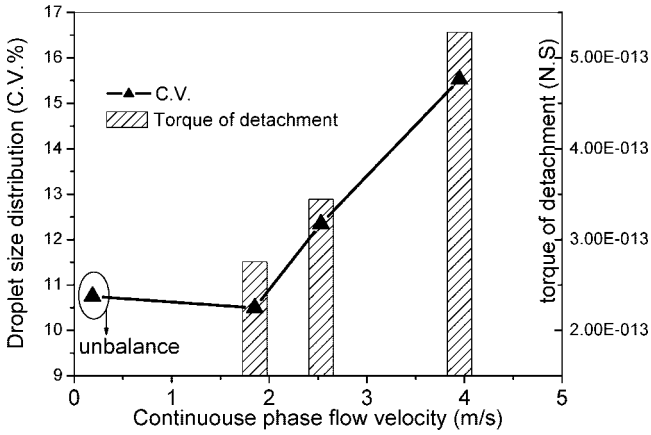

Figure 4. Influence of the velocity of the continuous phase flow on droplet size distribution by experiment and detachment torque analysis.

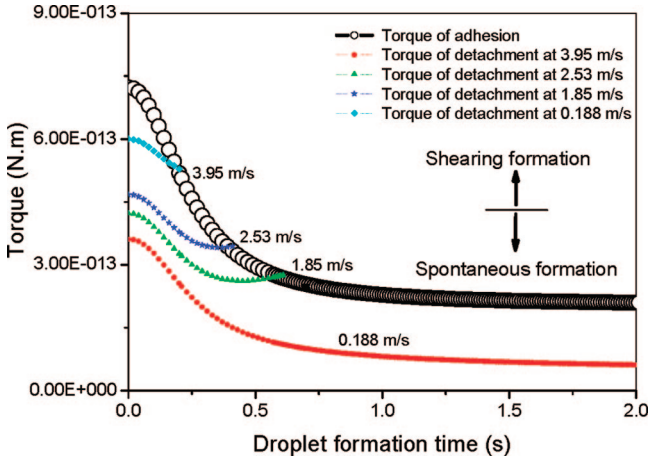

Figure 5. Development of torques on a global droplet at different velocities of continuous phase flow (operating conditions: dispersed phase, soybean oil; continuous phase, 2% SDS aqueous solution; and transmembrane pressure, 8 kPa).

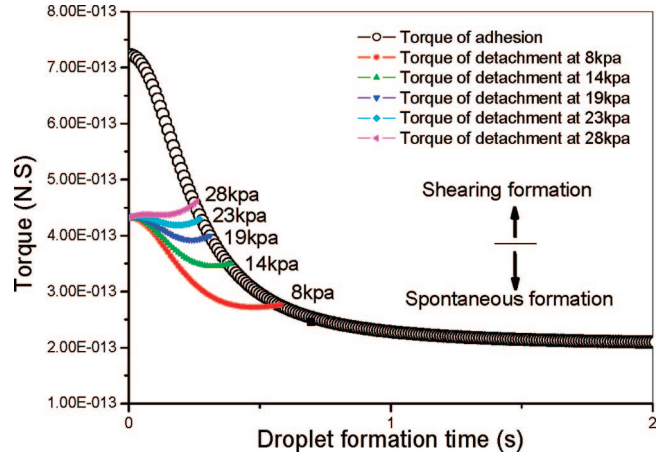

Figure 6. Development of torques on a global droplet at different transmembrane pressures, at the following operating conditions: dispersed phase, soybean oil; and continuous phase, 2% SDS aqueous solution, with a flow rate of 1.85 m/s.

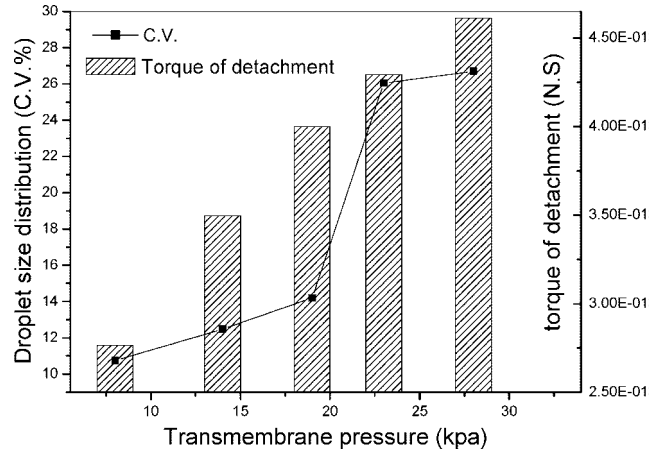

Figure 7. Influence of transmembrane pressure on droplet size distribution by experiment and detachment torque prediction.

m/s to 3.95 m/s, the balance point of detachment torques also continues to rise upward. From the increase in detachment torque at the balance point, it can be speculated that droplet detachment had a tendency to be controlled by the mechanism of shearing formation and the uniformity of emulsion became worse as the continuous phase flow rate increased. Another case should be noted: the two torques can never reach the balance point at a low continuous phase flow rate of 0.188 m/s, as shown in Figure 5. It was speculated that the detachment of droplets is driven totally by the mechanism of STB and it happens before the torques become balanced. Figure 4 also compared the relationship between the distribution of droplet size and the related predicted torques at the balance point. A general tendency was found that the emulsion uniformity (CV, expressed as a percentage) was spoiled at large detachment torques (at the balance point) as the continuous flow rate increased.

Based on different balance points of torque, droplet detachment can be divided into three cases:

Case i: torque of detachment≪ torque of adhesion, and they will never become balanced, as shown in Figure 5 at a low velocity of continuous phase flow (0.188 m/s). This case is speculated that the droplet detachment is driven by the mechanism of STB.

Case ii: torque of detachment = torque of adhesion, but the torque of detachment is still small and both the mechanisms of STB and SHE act. At this case, although both torques reach the balance point, a droplet still has a distorting and necking stage and continues to grow before it totally breaks off;

Case iii: torque of detachment = torque of adhesion, but, at this time, the balance torque of detachment is large enough to drag droplets away from the pore immediately and necking stage can be neglected. Obviously, the mechanism of SHE acts at this case. The aforementioned experimental results showed that if the operation conditions were controlled in cases (i) and (ii), a relatively uniform emulsion would be produced.

3.4. Influence of Transmembrane Pressure on Emulsion Uniformity. Another parameter with a strong influence on droplet size distribution is transmembrane pressure, which controls the flux rate of dispersed phase across the membrane channel and the development of detachment torque (see section 3.2 (ii)). Figure 6 shows that the detachment torque curves rose upward as the transmembrane pressures increased, and intersected with adhesion torque at the earlier and larger balance point. Therefore, it was speculated that a high transmembrane pressure would lead to the detachment mechanism of SHE and a polydisperse emulsion. The tendency of droplet size distribution observed under different emulsification pressure proves the aforementioned speculation. Experiments (see Figure 7) reveal that the increase in transmembrane pressure resulted in the formation of a polydisperse emulsion. When the dispersed-phase transmembrane pressure increased from the critical pressure (8 kPa) to 14 kPa, the CV value increased slightly from 11% to

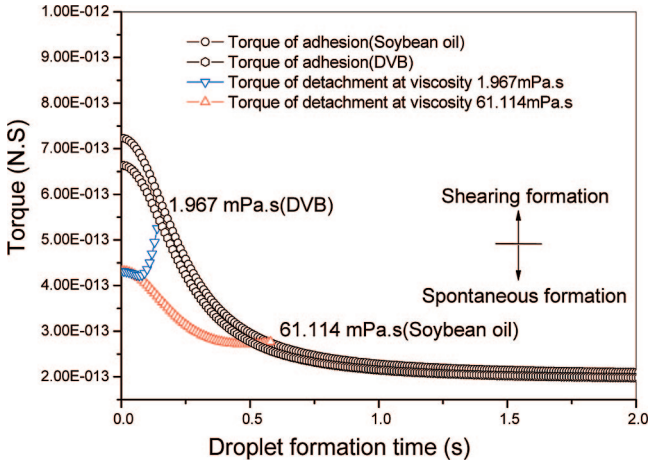

Figure 8. Development of torque on a global droplet at different viscosities of the dispersed phase (operating conditions: continuous phase, 2% SDS aqueous solution, with a flow rate of 1.85 m/s; and transmembrane pressure, 8 kPa).

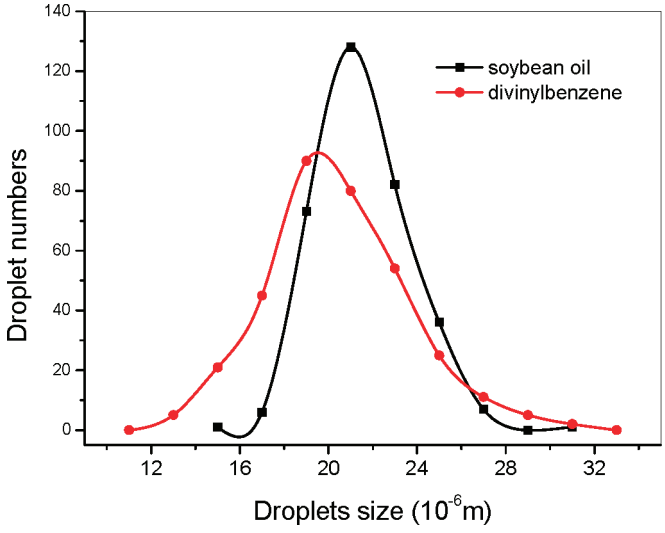

Figure 9. Droplet size distributions of the dispersed phase with different viscosities.

14%, and then reached a value of >26% when the transmembrane pressure was increased to 28 kPa.

3.5. Influence of Viscosity of the Dispersed Phase on Emulsion Uniformity. To compare the influence of the viscosity of the dispersed phase, two systems of dispersed-phase divinylbenzene and soybean oil were selected, because they have different viscosity but similar dynamic interfacial tension and density. The calculation of torques in Figure 8 showed that torques of the dispersed phase with high viscosity would get to balance later, which implied that droplet break from the pores was more easily and had a tendency to spontaneous experience the detachment mechanism and the production of a uniform emulsion. The aforementioned speculations can be demonstrated by emulsification experiments in Figure 9, where a droplet of soybean oil with high viscosity has a narrower size distribution than divinylbenzene with low viscosity.

3.6. Influence of Emulsifiers or Stabilizer on Emulsion Uniformity. Dispersants (such as emulsifiers and stabilizer) dissolved in continuous phase also play critical roles in membrane emulsification. First, they can quickly decrease the interfacial tension between dispersed-phase and continuous phase by adsorption at newly formed interface of droplet, and thus depress the critical transmembrane pressure in emulsification operation. Second, dispersants can restrain coalescence and aggregation between emulsion droplets. SDS, Tween20, and PVA are three typical dispersants that often are used in SPG membrane emulsification.[18,27,28] When SDS, with the highest surface activity, was used, the interfacial tension declines very fast and arrived at a low equilibrium value.[18] When stabilizer PVA was used, the interfacial tension cannot be decreased effectively, as in the case of SDS and Tween20, although it presents the best stabilizing ability in droplet suspension.[27] Because the interfacial tension force is a major force holding the droplet at the membrane pore, the dispersants that strongly lower the interfacial tension can help the droplet detach more easily from the membrane pore and, thus, facilitates droplet detachment as a spontaneous mechanism. Hence, we considered that SDS had more potential to obtain a uniform emulsion, and, comparatively, PVA more likely led to shearing detachment behavior and produced a polydisperse emulsion.

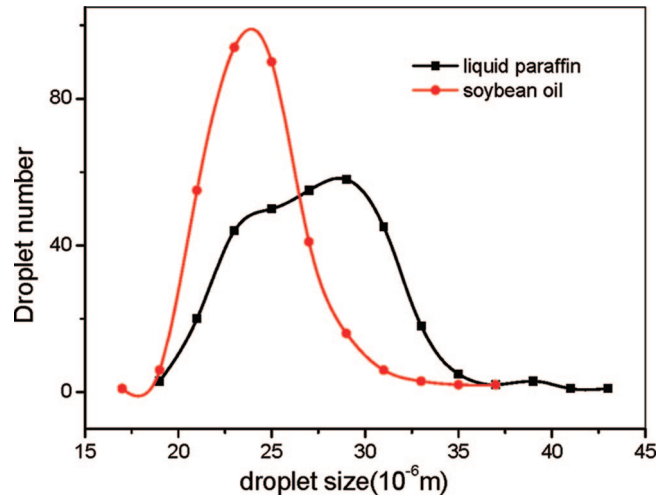

Figure 10. Droplet size distribution of different dispersed phases using PVA as a stabilizer.

We found that this tendency was dependent on the initial interfacial tension between two phases (i.e., the interfacial tension between the dispersed phase and pure water). When soybean oil with a low o/w interfacial tension (17 mN S) was used as a dispersed phase, even the PVA stabilizer can produce a uniform emulsion, and when paraffin with a higher o/w interfacial tension (46 mN S) as the dispersed phase, polydisperse emulsion was produced as shown in Figure 10. Torque calculation is described in Figure 11, and this figure shows that a larger initial interfacial tension of paraffin caused the rise of the adhesion torque curve and the balance point of the torques, which resulted in more polydispersity in the final emulsion.

Consequently, the influence of the type of dispersant on the droplet size distribution was more visible and comparable when paraffin was used as the dispersed phase, as shown in Figures 12 and 13. Emulsifiers such as SDS, which could reduce the interfacial tension, more deeply required a smaller detachment torque for balance. Accordingly, spontaneous droplet formation was facilitated, and a uniform emulsion was produced.

4. Conclusion

This work presented an analytical approach about different influences of process parameters, such as physical properties of a phase (viscosity, interfacial tension) and operationg conditions (e.g., transmembrane pressure shear stress), on emulsion uniformity in SPG membrane emulsification. Such effects in emulsification experiments under cross-flow conditions

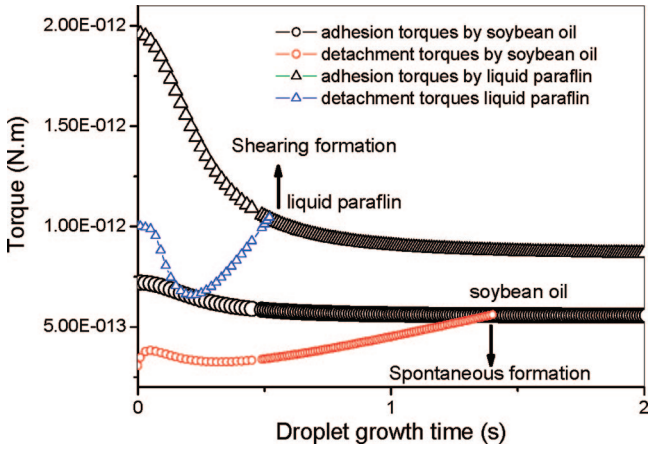

Figure 11. Development of torque on a global droplet by different dispersed phases, using PVA as a stabilizer (operating conditions: continuous phase flow rate, 0.94 m/s; continuous phase, 2% PVA aqueous solution; critical transmembrane pressure, 13 kPa for soybean oil and 24 kPa for paraffin).

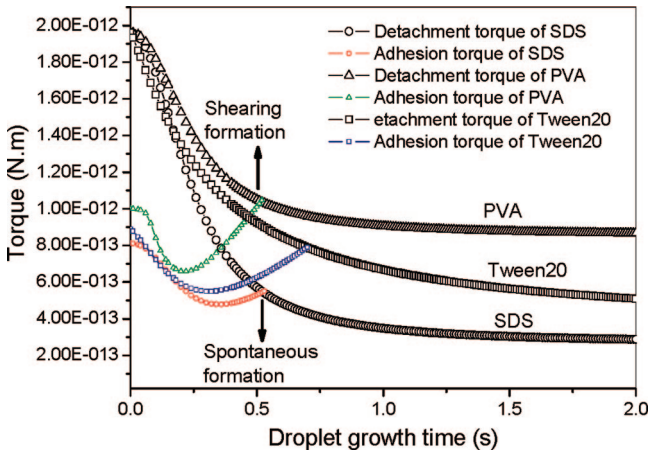

Figure 12. Development of torque on a global droplet of paraffin using SDS, Tween20, and PVA as emulsifiers and stabilizers (operating conditions: continuous phase flow rate, 0.94 m/s; continuous phase, 2% emulsifier aqueous solution; and transmembrane pressure, 14 kPa for SDS, 18 kPa for Tween20, and 29 kPa for PVA).

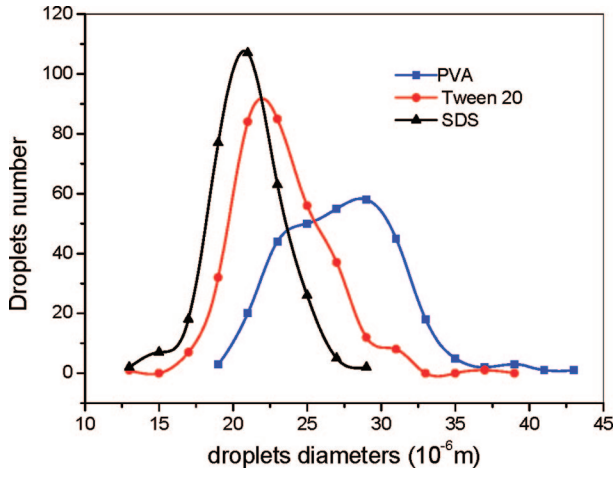

Figure 13. Droplet size distribution of paraffin, using SDS, Tween20, and PVA as emulsifiers and stabilizers.

were discussed experimentally and predicted by a theoretical model of torque balance. The model was constructed by interfacial tension dynamics, Darcy's law, and the cross-flow equation in a channel. The input parameters consisted of three groups: phase parameters, membrane parameters, and operation parameters. The output is the variable force torques in the droplet formation process. Based on the criteria that droplet spontaneous formation is a major mechanism to form a uniform emulsion, and by comparison of detachment torque and adhesion torque, one can easily determine how the input parameters affect the droplet detachment mechanisms and, thus, its uniformity. The experimental phenomena show a good coincidence with the predicted tendencies of the model. The following conditions are determined to facilitate uniform droplet formation: (1) low cross-flow velocity of the continuous phase; (2) low transmembrane pressure; (3) high viscosity of the dispersed phase; and (4) an emulsifier with great ability to decrease interfacial tension.

Although the aforementioned approaches cannot provide an exact value of droplet size distribution, the tendency for emulsion uniformity is predictable and controllable, which is significant for optimization of the operating conditions, screening of phase recipes suitable for emulsification, and even scaling up in pilot membrane emulsification.

Acknowledgment

Thanks for the support of National Natural Science Foundation of China (No. 20536050, 20221603, and 20636010), and the Chinese Academy of Sciences. We also are thankful for discussions with the cooperate research group of Unilever.

Nomenclature

γ_0 = interfacial tension between pure water and dispersed phase
γ_e = mesoequilibrium interfacial tension
d_{dr} = droplet diameter ($\times 10^{-6}$ m)
H = height of droplet
V_d = the volume of droplet (m^3)
d_p = membrane pore diameter ($\times 10^{-6}$ m)
A_p = cross-sectional area of the droplet neck at the pore (m^2)
ξ = pore tortuosity
D = inner diameter of membrane (m)
L = membrane thickness (m)
P_{ef} = effective transmembrane pressure (Pa)
P_{trm} = transmembrane pressure (Pa)
P_γ = capillary pressure (Pa)
P_γ^0 = critical transmembrane pressure (Pa)
Q_{dr} = dispersed phase flow rate through the pore (m^3/s)
u_d = average velocity of the dispersed phase (m/s)
u_c = average velocity of continuous phase (m/s)
μ_d = viscosity of the dispersed phase (Pa·s)
μ_c = viscosity of the continuous phase (Pa·s)
γ = interfacial force (N/m)
ρ = density (kg/m^3)
T_w = wall shear stress (Pa)
F_γ = interfacial tension force (N)
F_{sp} = static pressure difference force (N)
F_{cf} = crosslow drag force (N)
F_{dl} = dynamic lift force (N)
F_{BG} = buoyancy force (N)
F_m = linear momentum force (N)
$T_{adhesion}$ = torque of adhesion (N·m)
$T_{detachment}$ = torque of detachment (N·m)

Literature Cited

(1) Nakashima, T.; Shimizu, M.; Kukizaki, M. Particle control of emulsion by membrane emulsification and its applications. *Adv. Drug Delivery Rev.* **2000**, *45*, 47.

(2) Gijsbertsen-Abrahamse, A. J.; van der Padt, A.; Boom, R. M. Status of cross-flow membrane emulsification and outlook for industrial application. *J. Membr. Sci.* **2004**, *230*, 149.

(3) Li, X. N.; Sun, H. H.; Ma, G. H.; Su, Z. G. Rapid Purification of Huperzine A and B with Two Polystyrene based Resins by Preparative Low-Pressure Liquid Chromatography. *J. Liq. Chromatogr.* **2006**, *29*, 569.

(4) Lambrich, U.; Schubert, H. Emulsification using microporous systems. *J. Membr. Sci.* **2005**, *257*, 76.

(5) Schroder, V.; Schubert, H. Production of emulsions using microporous, ceramic membranes. *Colloids Surf. A* **1999**, *152*, 103.

(6) Vladisavljevic, G. T.; Schubert, H. Preparation and analysis of oil-in-water emulsions with a narrow droplet size distribution using Shirasu-porous-glass (SPG) membranes. *Desalination* **2002**, *144*, 167.

(7) Gijsbertsen-Abrahamse, A. J.; van der Padt, A.; Boom, R. M. Influence of membrane morphology on pore activation in membrane emulsification. *J. Membr. Sci.* **2003**, *217*, 141.

(8) Vladisavljevic, G. T.; Schubert, H. Influence of process parameters on droplet size distribution in SPG membrane emulsification and stability of prepared emulsion droplets. *J. Membr. Sci.* **2003**, *225*, 15.

(9) Vladisavljevic, G. T.; Schubert, H. Preparation and analysis of oil-in-water emulsions with a narrow droplet size distribution using Shirasu-porous-glass (SPG) membranes. *Desalination* **2002**, *144*, 167.

(10) Luca, G. D.; Sindona, A.; Giorno, L.; Drioli, E. Quantitative analysis of coupling effects in cross-flow membrane emulsification. *J. Membr. Sci.* **2004**, *229*, 199.

(11) De Luca, G.; Di Renzo, A.; Di Maio, F. P.; Drioli, E. Modeling droplet formation in cross-flow membrane emulsification. *Desalination* **2006**, *199*, 177.

(12) De Luca, G.; Di Maio, F. P.; Di Renzo, A.; Drioli, E. Droplet detachment in cross-flow membrane emulsification: Comparison among torque- and force-based models. Chem. Eng. Process. 2007, in press.

(13) Rayner, M.; Trägårdh, G.; Trägårdh, C.; Dejmek, P. Using the Surface Evolver to model droplet formation processes in membrane emulsification. *J. Colloid Interface Sci.* **2004**, *279*, 175.

(14) Rayner, M.; Trägårdh, G.; Trägårdh, C. The impact of mass transfer and interfacial expansion rate on droplet size in membrane emulsification processes. *Colloids Surf. A.* **2005**, *266*, 1.

(15) Kobayshi, I.; Mukataka, S.; Nakajuma, M. CFD simulation and analysis of emulsion droplet formation from straight through microchannels. *Langmuir* **2004**, *20*, 9868.

(16) van der Graaf, S.; Nisisako, T.; Schroen, C. G. P. H.; van der Sman, R. G. M.; Boom, R. M. Lattice Boltzmann Simulations of Droplet Formation in a T-Shaped Microchannel. *Langmuir* **2006**, *22*, 4144.

(17) Lian, G. P.; Jousse, F.; Janes, R.; Menech, M. D. Modeling the Formation and Flow of Multiphase Droplets in Microfluidic Devices. In *Chemical Engineering Research Trends*; Nova Science Publishers: Hauppauge, NY, 2007; Chapter 7.

(18) Schroder, V.; Behrend, O.; Schubert, H. Effect of Dynamic Interfacial Tension on the Emulsification Process Using Microporous, Ceramic Membranes. *J. Colloid Interface Sci.* **1998**, *202*, 334.

(19) Hua, X. Y.; Rosen, M. J. Dynamic surface tension of aqueous surfactant solutions, I. Basic Parameters. *J. Colloid Interface Sci.* **1988**, *124*, 652.

(20) Yasuno, M.; Nakajima, M.; Iwamoto, S.; Maruyama, T.; Sugiura, S.; Kobayashi, I.; Shono, A.; Satoh, K. Visualization and characterization of SPG membrane emulsification. *J. Membr. Sci.* **2002**, *210*, 29.

(21) Kobayashi, I.; Nakajima, M.; Mukataka, S. Preparation characteristics of oil-in-water emulsions using differently charged surfactants in straight-through microchannel emulsification. *Colloids Surf. A.* **2003**, *229*, 33.

(22) Kobayashi, I.; Nakajima, M. Silicon Array of Elongated Through-Holes for Monodisperse Emulsion Droplets. *AIChE J.* **2002**, *48*, 1639.

(23) Sugiura, S.; Nakajima, M.; Iwamoto, S.; Seki, M. Interfacial Tension Driven Monodispersed Droplet Formation from Microfabricated Channel Array. *Langmuir* **2001**, *17*, 5562.

(24) Kobayashi, I.; Mukataka, S.; Nakajima, M. Production of Monodisperse Oil-in-Water Emulsions Using a Large Silicon Straight-Through Microchannel Plate. *Ind. Eng. Chem. Res.* **2005**, *44*, 5852.

(25) Xu, J. H.; Luo, G. S.; Chen, G. G.; Wang, J. D. Experimental and theoretical approaches on droplet formation from a micrometer screen hole. *J. Membr. Sci.* **2005**, *266*, 121.

(26) Wang, Z.; Wang, S. C.; Schroeder, V.; Schubert, H. Influence of fluid flow on forces acting on droplet and emulsification results in membrane emulsification process. *J. Chem. Ind. Eng. (China)* **1999**, *50*, 505.

(27) Yuyama, H.; Watanabe, T.; Ma, G. H.; Nagai, M.; Omi, S. Preparation and analysis of uniform emulsion droplets using SPG membrane emulsification technique. *Colloids Surf. A* **2000**, *168*, 159.

(28) van der Graaf, S.; Schroën, C.G.P.H.; van der Sman, R. G. M.; Boom, R. M. Influence of dynamic interfacial tension on droplet formation during membrane emulsification. *J. Colloid Interface Sci.* **2003**, *225*, 15.

Received for review January 8, 2008
Revised manuscript received March 9, 2008
Accepted March 11, 2008

IE8000315